Hadamard Ratio Spectrum Sensing in Realistic CRN Channels

Lucas Claudino, Ricardo Kobayashi and Taufik Abrão

***Abstract*— Cognitive radio networks (CRN) are constantly in need for new technologies able to improve their performance. Hence, study of new spectrum sensing (SS) techniques and devices is extremely important for a development of more accurate and sensible devices. The Hadamard ratio-based spectrum sensor (HrS) is a robust method able to accurately sense the presence of a wireless signal by applying a statistic test based on maximum-likelihood (ML) of collected signal data. A further performance analysis of HrS techniques under realistic MIMO (Multiple-Input and Multiple-Output) fading channels is the contribution of this work. As a result, simulations aim to demonstrate its efficiency and how applicable would be a HrS procedure when inserted in real non-line-of-sight (NLOS) MIMO channel scenarios.**

***Keywords*— Cognitive Radio; Spectrum Sensing; Hadamard Ratio; Rayleigh fading; Path loss.**

I. INTRODUCTION

Cognitive radio (CR) technologies aim to optimize spectrum access by proposing methods for a licensed user (PU, primary user) to share the spectrum with a secondary user (SU). Many techniques try to detect white-spaces (in spectrum, time or space) sensing whether a primary signal is present or not and then try to access them so both CR and PU use the spectrum band either at different time or frequency slots or in different geographic regions [1]. Several methods can be used for sensing those white-spaces, such as energy detection sensing (EnS), coherent sensing, cyclostationary-based sensing, matched filter sensing [2], [3], among others.

A few authors [4]–[6] have devoted a long time to study, develop and prove statistical models for a new and promising technology based on generalized likelihood ratio test (GLRT), known as HrS applied to CR; however, the majority of results are valid for AWGN channels, which represents a simplified condition for real wireless channel scenarios. This article comes to contribute to SS in cognitive radio by analyzing the HrS under realistic wireless communication channels. The proposed HrS detector has been characterized by Monte-Carlo simulations considering Rayleigh fading and path-loss channels effects, as well as thermal interference, aiming to understand how this technology would behave if inserted in a real cognitive radio hardware.

This paper firstly formulates important signals of a typical HrS scenario, then basic HrS theory, operation and sensing methods and merit figures are properly calculated and explained. Section III analyses performance of a HrS under Rayleigh fading, path loss and AWGN channels via probabilities of detection (P_d) and false alarm (P_f) for different cases. A further extension of works in [5], [6] has been done. In order tho show the benefits of HrS, a comparison between HrS and other former sensors has been simulated based on an accurate estimation previously formulated. Additionally, differently from [5], a realistic channel has been considered. Also, a further analysis of sample complexity for HrS operating in fading channels has been considered as another point to confirm the sensor's robustness. Finally, results, future study possibilities and applications are discussed in section IV.

Notation: $\mathcal{L}(\cdot)$ denotes the likelihood function, P_d is probability of detection and P_f probability of false alarm. An scalar variable is denoted as x, while $\mathbf{x}$ is a vector and $\mathbf{X}$ represents a matrix form. $\Gamma(\cdot)$ is the gamma function.

II. HADAMARD RATIO-BASED ROBUST SPECTRUM SENSING

Hadamard ratio test is a robust method to provide signal detection in multivariate analysis which is able to deal with non-independent and identically distributed (non-*i.i.d.*) noise [5]. Recently, Hadamard Ratio test has been exploited for robust SS in CR [4], [6].

For the proposed problem, a transmission with n_T primary antennas not necessarily co-located is considered. At receiver's side, N samples are received by M SU's antennas under two circumstances: H_0 when PUs are absent and H_1 when they are active. Hence, a received

L. Claudino, R. Kobayashi and T. Abrão. Department of Electrical Engineering, Londrina State University, Londrina-PR, Brazil, E-mails: lsclaudino@gmail.com, taufik@uel.br, ricardokobayashi_5@hotmail.com.

signal can be written as:

$$\mathbf{x}[n] = \begin{cases} \boldsymbol{\eta}[n] & : \mathrm{H}_0 \\ \mathbf{H}\mathbf{s}[n] + \boldsymbol{\eta}[n] & : \mathrm{H}_1 \end{cases}. \quad (1)$$

Notice: $n = 1, 2, \ldots, N$ is the discrete-time index for all signals. Also, the received signal $\mathbf{x}[n]$ has M complex entries, one for each received antenna, i.e., $\mathbf{x}[n] \in \mathbb{C}^M$. Furthermore, $\mathbf{H} \in \mathbb{C}^{M \times n_T}$ is the MIMO channel matrix. Transmitting signals are denoted as $\mathbf{s}[n] \in \mathbb{C}^{n_T}$, where each entry stores a signal from one of the n_T users, considering $s_i \sim \mathcal{N}\left(0, \sigma^2_{s_i}\right)$. Finally, noise at receiver side is represented by $\boldsymbol{\eta}[n] \in \mathbb{C}^M$, where $\sigma^2_{\eta_i}$ is the unknown noise variance on each antenna, i.e., , $\eta_i[n] \sim \mathcal{N}\left(0, \sigma^2_{\eta_i}\right)$.

If radio frequency chains on receiver's side are uncalibrated, noise will be different at each antenna, consequently: $\sigma^2_{\eta_i} \neq \sigma^2_{\eta_j}$ for $i \neq j$. Thus, the sensing problem is to actually determine if $\mathbf{X} = [\mathbf{x}[1] \cdots \mathbf{x}[N]]$ is composed only by noise or both signal plus noise.

Fig. 1 depicts a block diagram for the proposed HrS. Firstly, a transmitter (PU) generates data string $\mathbf{s}[n]$ which is transmitted over a MIMO channel. At the SU, ML estimator is obtained by calculating the received signal's covariance matrix under both hypothesis H_0 and H_1, which allows the SS device to determine statistics of a test variable ξ. Finally, the spectrum status is determined based on a preset threshold: if $\xi < \gamma \rightarrow \mathrm{H}_1$ or if $\xi > \gamma \rightarrow \mathrm{H}_0$.

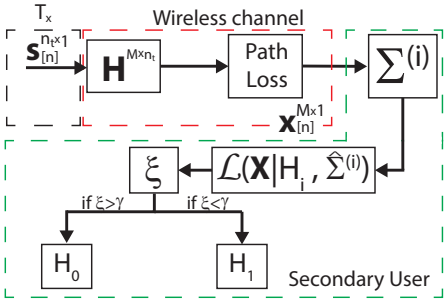

Fig. 1. Block diagram for a generic HrS.

1) GLRT Derivation: The observation set (1) is assumed to be Gaussian distributed and conditioned to the ith $(i = 0, 1)$ hypothesis test, $\mathbf{x}[n]|\mathrm{H}_i \sim \mathcal{N}\left(0, \boldsymbol{\Sigma}^{(i)}\right)$, with $\boldsymbol{\Sigma}^{(i)} \in \mathbb{C}^{M \times M}$ being the covariance matrix defined as:

$$\boldsymbol{\Sigma} = \mathbb{E}\left[\mathbf{X}\mathbf{X}^H\right] = \begin{bmatrix} \Sigma_{11} & \Sigma_{12} & \cdots & \Sigma_{1M} \\ \Sigma_{21} & \Sigma_{22} & \cdots & \Sigma_{2M} \\ \vdots & \vdots & \ddots & \vdots \\ \Sigma_{M1} & \Sigma_{M2} & \cdots & \Sigma_{MM} \end{bmatrix} \quad (2)$$

and $\Sigma_{ij} = \Sigma^H_{ij} = \mathbb{E}\left[\mathbf{x}^H_i \mathbf{x}_j\right]$. The matrix $\boldsymbol{\Sigma}$ expresses independence between every pair of channels [7].

Indeed, $\boldsymbol{\Sigma}^{(0)} = \mathrm{diag}(\sigma^2_{\eta_1}, \cdots, \sigma^2_{\eta_M})$ represents the noise-only observation hypothesis H_0 and $\boldsymbol{\Sigma}^{(1)}$ is a non-diagonal matrix representing covariance between every pair of secondary antennas under hypothesis H_1.

According to [7], the conditional likelihood function of $\mathbf{X}$ under H_i hypothesis may be defined as:

$$\mathcal{L}\left(\mathbf{X}\,|H_i\right) = \frac{\exp\left\{-N \cdot \mathrm{tr}\left[\left(\boldsymbol{\Sigma}^{(i)}\right)^{-1} \widehat{\boldsymbol{\Sigma}}\right]\right\}}{\pi^{MN}\left|\boldsymbol{\Sigma}^{(i)}\right|^N} \quad (3)$$

Using ML estimation procedure, the derivative of (3) is set to zero in order to find the ML estimator of $\boldsymbol{\Sigma}^{(0)}$ and $\boldsymbol{\Sigma}^{(1)}$ as $\widehat{\boldsymbol{\Sigma}}^{(0)} = \mathrm{diag}(\widehat{\boldsymbol{\Sigma}})$ and $\widehat{\boldsymbol{\Sigma}}^{(1)} = \widehat{\boldsymbol{\Sigma}}$, where $\widehat{\boldsymbol{\Sigma}} = (1/N)\sum_{n=1}^{N} \mathbf{x}[n]\mathbf{x}[n]^H$ is the sample covariance matrix. Finally, HrS's GLR for is written as:

$$\xi = \frac{\max\limits_{\boldsymbol{\Sigma} \in H_0} \mathcal{L}\left(\mathbf{X}|\mathrm{H}_0, \boldsymbol{\Sigma}^{(0)}\right)}{\max\limits_{\boldsymbol{\Sigma} \in H_1} \mathcal{L}\left(\mathbf{X}|\mathrm{H}_1, \boldsymbol{\Sigma}^{(1)}\right)} \quad (4)$$

Hence, the Hadamard Ratio is finally obtained by applying ML estimators and (3) into (4), i.e.:

$$\xi = \frac{\left|\widehat{\boldsymbol{\Sigma}}^{(1)}\right|}{\left|\widehat{\boldsymbol{\Sigma}}^{(0)}\right|} \quad (5)$$

which is bounded by $[0, 1]$, once $\left|\widehat{\boldsymbol{\Sigma}}\right|$ dramatically decreases in presence of primary signals and presents its maximum value of $\left|\mathrm{diag}(\widehat{\boldsymbol{\Sigma}})\right| = \left|\widehat{\boldsymbol{\Sigma}}^{(0)}\right|$ when under H_0. Hence, H_1 is sensed if ξ is smaller than a chosen threshold γ, otherwise, H_0 occurs:

$$\xi \underset{H_1}{\overset{H_0}{\gtrless}} \gamma \quad (6)$$

Exact distribution for this GLRT may assume complex values; however, its moments can be straightforwardly expressed using a moment approximation. The test statistic ξ can be approximated by a beta distributed random variable (*r.v.*) defined in $[\theta_1, \theta_2]$, with shaping parameters α and β and a probability density function *p.d.f.*:

$$f(x) \simeq \begin{cases} \dfrac{(x-\theta_1)^{\alpha-1}(\theta_2 - x)^{\beta-1}}{B(\alpha, \beta)}, & \theta_1 \leq x \leq \theta_2 \\ 0, & \text{otherwise,} \end{cases} \quad (7)$$

where $B(\alpha, \beta) = \dfrac{\Gamma(\alpha)\Gamma(\beta)}{\Gamma(\alpha + \beta)}$ is the Beta Function.

Based on methods of [8]–[10], first and second moments of ξ can be calculated. Beta distribution is then used to perform a moment matching, so probabilities of detection and false alarm are accurately estimated [5].

Indeed, authors of [5] and [6] have precisely derived exact moments of ξ in order to provide a more accurate approximation for the test's distribution. For simulation purposes, it is valid to numerically calculate moments from available signal samples and use them as a beta distributed *r.v.*

Probability of false alarm for ξ is defined as $P_f \triangleq \Pr\{\xi < \gamma \,|\mathrm{H}_0\}$ and, given the c.d.f. of a beta *r.v.* bounded by $[0,1]$, P_f is calculated as:

$$P_f \simeq \int_0^{\gamma} \frac{1}{B(\alpha_0,\beta_0)} z^{\alpha_0-1}(1-z)^{\beta_0-1}dz = \frac{B_x(\alpha_0,\beta_0)}{B(\alpha_0,\beta_0)} = F(\gamma) \quad (8)$$

where $B_x(\alpha_0,\beta_0) = \int_0^x z^{\alpha_0-1}(1-z)^{\beta_0-1}dz$ is the incomplete Beta function, α_0 and β_0 are shape parameters for H_1 approximated with the first two positive moments of ξ.

Similarly, probability of detection for ξ $\left(P_d \triangleq \Pr\{\xi < \gamma \,|\mathrm{H}_1\}\right)$ was derived in [5] via moment matching strategy:

$$P_d \triangleq Pr\{\xi < \gamma \,|\mathrm{H}_1\} = \frac{B_x(\alpha_1,\beta_1)}{B(\alpha_1,\beta_1)} = F(\gamma) \quad (9)$$

where shape parameters for hypothesis H_1, *i.e.*, α_1 and β_1 are obtained as function of the test statistic's first two negative moments.

III. Numerical Results

This section is devoted to compare and analyze performance of proposed HrS in realistic wireless channel scenarios. Most researches on HrS, have been done on performance analysis under AWGN channels [5], [6], [11], [12]; however, for future 5G networks and CR possibilities, SS performance must be analyzed in realistic MIMO channel scenarios, including path-loss influence, non-line-of-sight Rayleigh fading and shadowing effects.

Firstly, sensor's robustness must be tested and compared to other SS techniques. Indeed, based on results of [13], an Energy detector in realistic scenario has been considered as a comparison metric for analyzing HrS's performance.

AWGN channels represent a very simple and unrealistic approximation of real wireless channel scenarios. Hence, Clarke's fading model is deployed [14], [15] to create a Rayleigh fading channel matrix. This channel model not only is a more accurate representation of a wireless channel but also allows evaluation of user's mobility influence by inserting the maximum Doppler shift factor f_d. The constant f_d depends on user's velocity v and carrier frequency f_c, i.e., $f_d = \frac{v}{c} f_c$, where c is the light velocity. Hence, for slow fading channels, a pedestrian user with $f_d \approx 5$Hz has been considered, while for fast fading a vehicular user, $f_d \approx 100$Hz has been adopted.

TABLE I
Reference values used for simulations

Parameter	Value
Avg. PU power	$P_t \in [-100, -20]$dBm
PU-SU dist.	$d = 1000$m
Noise power	$P_{\text{noise}} = -100$dBm
SNR	SNR $\in [-3, 7]$dB
# samples	$N \in [32, 1024]$
# SU antennas	$M = 12$
# PU	$n_T = 5$
Doppler freq.	$f_d \in \{5, 200\}$Hz
Path-loss exponent	$\psi = 4$

Additionally, an average PU-SU separation d has been considered when calculating the path-loss effect, while the average transmitted power was set to operate in range $P_t \in [-100; -20]$ dBm. Table I contains reference values for channel and signal estimation used on simulations of this section. AWGN noise interference was modeled mainly as thermal effect with $P_{\text{noise}} = -100$dBm, which allows us to calculate the receiver's SNR dividing the received power by the noise power.

Fig. 2 compares the simulation results for both conventional EnS and Hadamard ratio SS techniques. All simulations have been done for $d = 1$km, fast fading $f_d = 200$Hz, $N = 128$, samples and other parameters according to Table I. In order to characterize the average CR system behavior, Monte-Carlo simulations with $\mathbf{10^6}$ realizations per performance point were proceeded, guaranteeing a confidence interval of 98% and maximum error of 5%.

Firstly, fig. 2 shows how harmful the channel is for an EnS detection. For an AWGN scenario, EnS has an expressive performance for $SNR = -3$dB; however, fading processes severely degrades its performance, once not even at $SNR = 7dB$ an acceptable detection rate is achieved. In contrast, proposed HrS has similar and satisfying performance under both AWGN and fading channels (red circled and blue dashed lines, respectively), which indicates a certain robustness to fading for HrS-based SS techniques.

Additionally, an analysis of user mobility effects on SS is also important. In this sense, a ROC (Receiver Operating Characteristics) comparison for transmissions under slow and fast fading illustrates this process of interference. A flat Rayleigh fading channel, i.e. $h_{ij} \sim$

$\mathcal{CN}(0,1)$[1], was considered. Also, channel matrix's elements were normalized not to affect signal's power, as it is the path loss task; thus, the constraint $\mathbb{E}\left[|h_{ij}|^2\right] = 1$ must be respected.

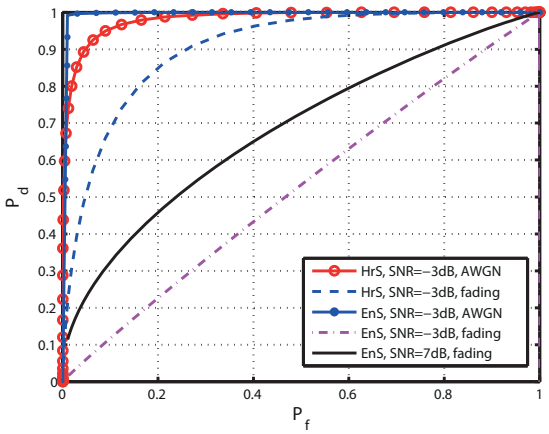

Fig. 2. ROC comparison for EnS and HrS.

For the next scenario, a wireless transmission under Rayleigh fading, path-loss and thermal noise effects will be considered as a scenario for analyzing influence of user's mobility and total number of samples used in SS. Two cases were considered: firstly a slow Rayleigh fading scenario and secondly a fast fading, where the channel is changing at every collected sample.

The performance of a HrS operating under different channel scenarios and a variable number of samples in range of $N \in [32, 1024]$ is presented on fig. 3. For this simulation experiment, the transmitting power was fixed to -20dBm, $M = 12$ antennas, $n_t = 5$ users and $d = 1000$m, which results in $SNR = 0$dB. The remaining parameters are set according to table I. Also, it is noteworthy mentioning that a *semilogx* scale has been used as an alternative to offer a better view of curves' behavior, once they would all be compacted at the upper left corner of a linear scale graphic.

Firstly, axes limits of fig. 3.a) show how HrS presents an excellent performance for slow fading cases. Additionally, the samples variation suggests the absence of an SNR wall for this case, once a small variation on sample complexity causes a minimal performance enhancement, but a double in sample complexity also doubles P_d.

A performance gap can be observed by comparing figs. 3.a) and 3.b). Despite performance degradations caused by fast fading, the HrS can still achieve a good performance even with a low number of samples. For example, at a 0dB SNR scenario, an acceptable performance for a SS device is already guaranteed with 1024

[1] $|h_{ij}|$ follows a Rayleigh distribution, while $\angle h_{ij}$ is uniformly distributed

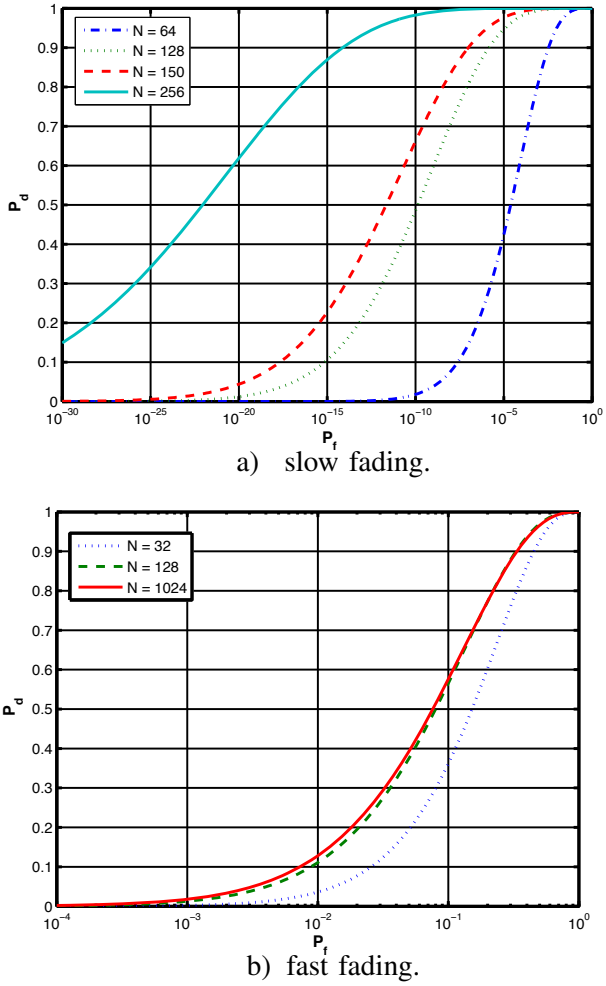

Fig. 3. ROC for a HrS with different sample complexities.

samples. Additionally, a closer look at fig. 3 suggests an SNR wall at $N \approx 128$ as performance improvements are negligible if more samples are used.

An average upper power limit of 10W for an urban cellular tower has been established by the Federal Communications Commission [16]. In case of a HrS, an average transmitting power of -10dBm was used for simulations of a sensor located 1km away; hence, HrS' performance under effect of fast fading channels, path-loss and AWGN noise interference is hold in strict accordance with requirements for realistic application scenarios, confirming the sensor's robustness for cognitive radio networks.

IV. Final Remarks

This paper aims to study a new and promising technology based on the well established likelihood theory for SS of cognitive radio networks: Hadamard ratio detector. Current literature for this technique is yet very limited, as it is based on studies of non-realistic AWGN scenarios. A few work on performance of HrS in realistic cases has

been done. Hence, an application of previous developed statistic theory was considered in this paper. Monte-Carlo simulations for HrS under Rayleigh multipath fading channels have been proceeded for wireless setups under effect of the path-loss.

Numerical results showed how basic detectors, such as EnS may de inefficient when operating in realistic scenarios. Additionally, HrS' robustness was proved via simulations of multipath fading channels, once a minimal degradation due to multiplicative effect of Rayleigh fading has been observed on performance figures of section III. Additionally, simulations considered Tx-Rx separation via inserting a model of path loss, so transmission power level limits could be tested for both EnS and HrS detectors.

A difference in performance of fast and slow fading channels was observed; however, both situations show an advantage of HrS: the low sample complexity. This first results strongly encourage us to believe HrS is prone to achieve high performance under real CRN channel scenarios. Indeed, considering realistic wireless channel scenarios (including path-loss effect with $\psi = 4$), HrS has demonstrated suitable performance in terms of ROC, achieving a $P_d \geq 0.95$ for a $P_f = 0.1$ under low number of samples in the range $128 \leq N \leq 1024$ and low signal-to-noise ratio, ranging $-3 \leq \text{SNR} \leq 0$ dB.

CR technology has been developed to allow systems to work with very low transmission power and achieve high performance levels. Even though path-loss effect showed to be harmful to CRs, power levels remain very low if compared to conventional cellular base stations and terminals. For example, according to the Federal Communications Commission, a transmission power operating with $P_t = 10\text{W}$ in urban regions is acceptable; our simulations showed that, if considering an average Tx-Rx separation $d = 1\text{km}$, spectral sensing device will operate with high level of SS detection $P_d \geq 0.9$ if PU is transmitting with $P_t \geq -20\text{dBm}$. Hence, the SS of CRs may be a technology able to significantly increase power efficiency of wireless transmissions.

Hence, this research enables many opportunities for further studies beyond optimization of cell configurations, performance of HrS in different and possibly even more realistic as well challenging CR scenarios and also identification of an optimal value of sample complexity and transmission power that enhances even more performance of CR networks.

REFERENCES

[1] G. Zhao, J. Ma, G. Li, T. Wu, Y. Kwon, A. Soong, and C. Yang, "Spatial spectrum holes for cognitive radio with relay-assisted directional transmission," *Wireless Communications, IEEE Transactions on*, vol. 8, no. 10, pp. 5270–5279, October 2009.

[2] E. Biglieri, A. Goldsmith, L. Greenstein, N. Mandayam, and H. V. Poor, *Principles of Cognitive Radio*. Cambridge, UK.: Cambridge University Press, 2012.

[3] A. G. Hernandes, R. T. Kobayashi, and T. Abrão, *Introduction to Cognitive Radio Networks and Applications*, 1st ed. Chapman and Hall/CRC Press, July 2016, ch. Spectrum Sensing Techniques in cognitive radio networks: Achievements and challenges, p. 42.

[4] J. Tugnait, "On multiple antenna spectrum sensing under noise variance uncertainty and flat fading," *Signal Processing, IEEE Transactions on*, vol. 60, no. 4, pp. 1823–1832, April 2012.

[5] L. Huang, Y. Xiao, H. C. So, and J. Fang, "Accurate performance analysis of hadamard ratio test for robust spectrum sensing," *Wireless Communications, IEEE Transactions on*, vol. 14, no. 2, pp. 750–758, Feb 2015.

[6] A. Mariani, A. Giorgetti, and M. Chiani, "Test of independence for cooperative spectrum sensing with uncalibrated receivers," in *Global Communications Conference (GLOBECOM), 2012 IEEE*, Dec 2012, pp. 1374–1379.

[7] N. Klausner, M. Azimi-Sadjadi, L. Scharf, and D. Cochran, "Space-time coherence and its exact null distribution," in *Acoustics, Speech and Signal Processing (ICASSP), 2013 IEEE International Conference on*, May 2013, pp. 3919–3923.

[8] A. Simaan M., H. Daniel W., and W. James R., "Fitting beta distributions based on sample data," in *Journal of Construction Engineering and Management*, vol. 120, no. 2, June 1994, pp. 288–305.

[9] N. L. Johnson, S. Kotz, and N. Balakrishnan, *Continuous Univariate Distributions*. Wiley-Interscience, 1995.

[10] M. T. Chao and W. E. Strawderman, "Negative moments of positive random variables," in *Journal of the American Statistical Association*, vol. 67, no. 338, June 1971, pp. 429–431.

[11] R. Lopez-Valcarce, G. Vazquez-Vilar, and J. Sala, "Multi-antenna spectrum sensing for cognitive radio: overcoming noise uncertainty," in *Cognitive Information Processing (CIP), 2010 2nd International Workshop on*, June 2010, pp. 310–315.

[12] D. Ramirez, G. Vazquez, R. Lopez Valcarce, J. Via, and I. Santamaria, "Detection of rank- p signals in cognitive radio networks with uncalibrated multiple antennas," *Signal Processing, IEEE Transactions on*, vol. 59, no. 8, pp. 3764–3774, Aug 2011.

[13] F. F. Digham, M. S. Alouini, and M. K. Simon, "On the energy detection of unknown signals over fading channels," in *Communications, 2003. ICC '03. IEEE International Conference on*, vol. 5, May 2003, pp. 3575–3579 vol.5.

[14] A. Goldsmith, *Wireless Communications*. New York, NY, USA: Cambridge University Press, 2005.

[15] G. L. Stuber, *Principles of Mobile Communication*. Springer, 2002.

[16] F. C. Commission, "Human exposure to radio frequency fields: Guidelines for cellular and pcs sites," Available at: http://transition.fcc.gov/cgb/consumerfacts/rfexposure.pdf, 2015.